

Dipole-flow disturbed by a circular inclusion of conductivity different from the background: From deterministic to a self-consistent analytical solution

Gerardo Severino ^{1,*}, Francesco De Paola ^{2,†} and Gerardo Toraldo ^{3,‡}

¹*Division of Water Resources Management, University of Naples - Federico II via Università 100 - I-80055, Portici (NA), Italy*

²*Division of Hydraulics, University of Naples - Federico II via Claudio 21 - I-80125, Napoli (NA), Italy*

³*Department of Mathematics and Physics, University of Campania - Luigi Vanvitelli viale Lincoln 5 - I-81100, Caserta (CE), Italy*



(Received 19 October 2021; accepted 31 May 2022; published 22 June 2022)

Steady dipole-flow through a porous medium, and disturbed by a circular inclusion Ω_0 of conductivity different from the background, is solved analytically. The solution is achieved by means of the circle theorem, which is reformulated to account for the entry/leave of mass and energy through the boundary $\partial\Omega_0$. It is shown that the governing potential is that which one would consider in absence of the disturbance supplemented with an *ad hoc* (fictitious) dipole laying inside Ω_0 . Besides the theoretical interest, the analytical solution is used to compute the effective conductivity K^{eff} , by means of the self-consistent approximation. Overall, K^{eff} is found to depend upon the flow configuration, and therefore it cannot be sought as a medium's property (nonlocality). In particular, K^{eff} depends upon the joint probability density function f of the conductivity and the distribution/size of the inclusions. Results, analyzed for a fairly general model of f , demonstrate that the coefficient of correlation ρ between the involved random fields is the key parameter characterizing the structure of K^{eff} . Indeed, the latter results larger or smaller than that of the background, depending on whether ρ is negative or positive, respectively. For $\rho = 0$, the effective conductivity is a local property and, in this case, one can apply the superposition principle with the homogeneous conductivity replaced by the geometric mean.

DOI: [10.1103/PhysRevFluids.7.064101](https://doi.org/10.1103/PhysRevFluids.7.064101)

I. INTRODUCTION

We consider a steady process driven by a dipole-type configuration, and we deal with a linear constitutive law, i.e.,

$$\mathbf{q}(\mathbf{x}) = -K \nabla h(\mathbf{x}), \quad (1)$$

relating the flux \mathbf{q} , at any position \mathbf{x} , to the gradient of the potential h through the coefficient K . Besides fluid mechanics, whose terminology shall be adopted in the sequel, there are other branches of physics (such as heat transfer and electromagnetism) accounting for a constitutive law with the same mathematical structure of (1). For example, it can be used to compute the steady temperature generated by isolated/distributed point sources [1], a setup that is instrumental to identify the thermal conductivity of materials. Still in the theory of heat transfer, the constitutive

*gerardo.severino@unina.it

†francesco.depaola@unina.it

‡gerardo.toraldo@unicampania.it

law (1) may serve to compute the temperature field in a region that is heated by a source located at a given point, and simultaneously cooled by a sink implanted into another point. In electrostatics, it is useful to compute the electric field in a region characterized by the presence of single and/or distributed positive and negative point charges [2]. In addition, it is also useful in addressing the first-order (dipole) approximation in the multipole expansion of the electric potential as determined by localized charges. Likewise, the model (1) is used to compute the magnetic field as generated by a current localized in a small (as compared to the length scale of interest) region of the space. In the study of planar waves, it serves to investigate how a signal emitted from a waveguide is detected by another one, after propagating through a dielectric of given permittivity. Finally, in the subsurface hydrology, it is often used for identification purposes (e.g., [3]) or *in situ* remediation strategies to clean up portions of polluted ground waters (e.g., [4,5]). As such, the problem at stake finds application in numerous fields of applied physics as well as reservoir engineering.

Potential theory has provided several analytical solutions for steady flows from/toward isolated and/or distributed sources by regarding the medium as homogeneous (see, e.g., [6]). A variation considers a source flow disturbed by a circular inclusion of conductivity $K_0 \neq 0$, and different from that of the background [7–9]. However, to the authors’ knowledge, an analytical solution for a dipole-flow through a circular inclusion of nonzero permeability has not been yet achieved.

Besides the theoretical interest, and its implication toward the applications in the classical hydrological engineering, dipole-flow disturbed by an inclusion of a different conductivity finds application in the effective theory of disordered media (an overview in the context of fluids can be found in [10]). In particular, here we are interested in the *effective conductivity* (EC), which is the parameter to be used in the average constitutive (Darcy) equation. The EC is computed by means of the *self-consistent approximation* (SCA) which is applied here to a dipole-flow. The physical model underlying the SCA regards the porous formation as a collection of numerous, homogeneous inclusions set at random in the space, and the fluctuation of the velocity field induced by each inclusion is computed by assuming that it is surrounded by a homogeneous matrix of unknown conductivity. Hence, the EC is computed by requiring that “it is equal to the conductivity of the medium as a whole” [11]. In spite of its approximate nature, it leads (unlike the perturbation approach; see, e.g., [12]) to a simple expression, free of any limitation upon the controlling parameter(s). Determining the EC in dipole-type flows, has been scarcely studied, its theoretical and practical importance notwithstanding [13,14]. To our knowledge there are only numerical studies simultaneously accounting for the aquifer’s heterogeneity and the nonuniformity of the flow pattern [15].

The problem at stake is very complex to solve numerically. The main difficulty is given by the strong coupling (especially in the zones surrounding the two singularities) between the spatial variability of Y and the nonuniformity of the flow. More precisely, to account for the very rapid variations of the velocity in the close vicinity of the singularities, a very dense grid is required, preventing *de facto* to achieve accurate solutions. This plays down significantly the ability of numerical solutions to solve accurately flow in a tiny zone surrounding the wells. Instead, analytical tools lead to simple (i.e., closed form) solutions which provide an explicit relationship between the input parameters and the model output, therefore giving physical insight to the problem at stake, without sorting to computationally heavy numerical simulations. In the present study, we show that, with the analytical expression derived in the first part, the EC can be computed even for a dipole-flow taking place in a heterogeneous porous formation.

II. CONFIGURATION OF THE FLOW PROBLEM AND ITS ANALYTICAL SOLUTION

We consider a steady flow taking place in an unbounded, two-dimensional domain \mathbb{R}^2 . For mathematical convenience, we deal with the complex variable z such that $x_1 \equiv \text{Re}(z)$ and $x_2 \equiv \text{Im}(z)$ being $\mathbf{x} \equiv (x_1, x_2) \in \mathbb{R}^2$. The velocity field is generated by a dipole, with the source and the sink at $(0, 0)$ and $(\ell, 0)$, respectively (Fig. 1). A circular inclusion Ω_0 of radius \mathcal{R}_0 is implanted with the center at z_0 . We assume that both the sink and the source lie outside Ω_0 , which is tantamount

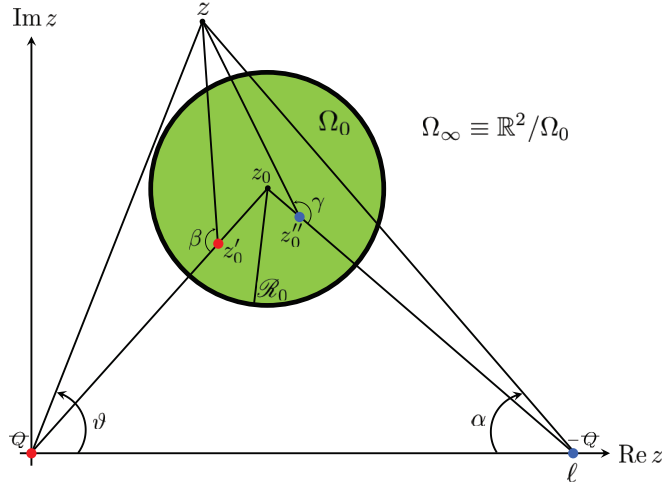


FIG. 1. Geometry of a dipole with the source (red) and the sink (blue) at $(0,0)$ and $(\ell, 0)$, respectively. The flow is disturbed by a circular inclusion Ω_0 of radius \mathcal{R}_0 and center z_0 . The positions z'_0 and z''_0 identify the fictitious dipole lying inside Ω_0 , whereas z is the current position

to requiring that $\mathcal{R}_0 < r_<$, being $r_< = \min\{|z_0|, |\ell - z_0|\}$ (Fig. 1). Hence, the flow domain consists of two subdomains, i.e., $\mathbb{R}^2 \equiv \Omega_\infty \cup \Omega_0$, with Ω_0 separating the portion of \mathbb{R}^2 lying within the inclusion from the external domain Ω_∞ . Our aim is the computation of the complex potential $w \equiv w(z)$ for such a configuration.

To illustrate the methodology, it is instrumental starting from the solution pertaining to an impermeable inclusion. Toward this aim, we make use of the circle theorem [16], stating that the complex potential resulting from the presence of an impermeable circular inclusion, of radius \mathcal{R}_0 and center in $(0,0)$, is given by

$$w(z) = w_*(z) + \bar{w}_*\left(\frac{\mathcal{R}_0^2}{z}\right), \quad (2)$$

where w_* is the potential of the flow field without disturbance (the “bar” symbol denotes complex conjugation). For a dipole flow of constant strength $\mathcal{Q}[\text{L}^2/\text{T}]$, the unperturbed potential is $w_*(z) = \mathcal{Q} \ln z - \mathcal{Q} \ln(z - \ell) + C$, being C a (generally complex) constant. In order to apply the circle theorem, we introduce the new variable $\zeta = z - z_0$ to shift the center z_0 of the inclusion to the origin of the ζ framework. As a consequence, the unperturbed potential writes as $w_*(\zeta) = \mathcal{Q} \ln(\zeta + z_0) - \mathcal{Q} \ln(\zeta + z_0 - \ell) + C$. Hence, application of (2) to this latter and moving back to the z framework lead to

$$w(z) = \mathcal{Q} \ln z - \mathcal{Q} \ln(z - \ell) + \mathcal{Q} \ln(z - z'_0) - \mathcal{Q} \ln(z - z''_0), \quad (3)$$

where we have set $z'_0 \equiv z_0 - \mathcal{R}_0^2/z_0$ and $z''_0 \equiv z_0 - \mathcal{R}_0^2/(z_0 - \ell)$. In addition, we have chosen $C = \mathcal{Q} \ln(1 - \ell/z_0)$. The potential (3) has a straightforward mechanical explanation: the obstacle Ω_0 acts *de facto* like an extra (fictitious) dipole, whose effect is that no mass leaves/enters through the boundary $\partial\Omega_0$ in order to fulfill the condition of impermeable inclusion. It is seen that z'_0 and $(0,0)$ are inverse points with respect to the circle Ω_0 [16], and the same is for z''_0 and $(\ell, 0)$. As a consequence, the two fictitious singularities z'_0 and z''_0 lie inside Ω_0 (Fig. 1).

We are in a position to adapt the above approach to a permeable inclusion of conductivity $K_0 \neq 0$. In this case, flow inside Ω_∞ is still generated by a dipole of strength \mathcal{Q} , whereas the system of fictitious sink/source is now characterized by a strength $\mathcal{Q}_\infty \neq \mathcal{Q}$ (to be determined):

$$w_\infty(z) = \mathcal{Q} \ln z - \mathcal{Q} \ln(z - \ell) + \mathcal{Q}_\infty \ln(z - z'_0) - \mathcal{Q}_\infty \ln(z - z''_0) + C_\infty. \quad (4)$$

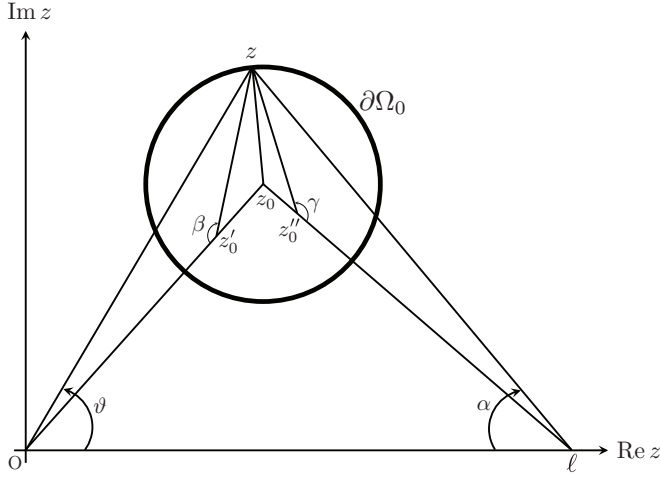


FIG. 2. Geometrical sketch pertaining to the fulfillment of the mass and energy conservation along the boundary $\partial\Omega_0$ of the inclusion.

Inside Ω_0 , flow is driven by a dipole of unknown strength $Q_0 \neq \mathcal{Q}$, i.e.,

$$w_0(z) = Q_0 \ln z - Q_0 \ln(z - \ell) + C_0. \quad (5)$$

The strengths Q_∞ and Q_0 are identified by requiring the continuity of the specific (per unit weight) energy $h \equiv h(\mathbf{x})$ ([L]), i.e.,

$$h(\mathbf{x}) = \begin{cases} h_\infty \equiv K_\infty^{-1} \operatorname{Re}(w_\infty), & \mathbf{x} \in \Omega_\infty, \\ h_0 \equiv K_0^{-1} \operatorname{Re}(w_0), & \mathbf{x} \in \Omega_0, \end{cases} \quad (6)$$

and of the stream function $\psi \equiv \psi(\mathbf{x})$:

$$\psi(\mathbf{x}) = \begin{cases} \psi_\infty \equiv \operatorname{Im}(w_\infty), & \mathbf{x} \in \Omega_\infty, \\ \psi_0 \equiv \operatorname{Im}(w_0), & \mathbf{x} \in \Omega_0, \end{cases} \quad (7)$$

along the boundary $\partial\Omega_0$. Unlike the case of impervious inclusion, the fictitious dipole behaves (i) to allow the flow passing through the inclusion, and (ii) to preserve energy and mass. It is convenient to represent the position of each singularity in polar coordinates as follows:

$$z = |z| \exp(i\vartheta), \quad z - z'_0 = |z - z'_0| \exp(-i\beta), \quad (8)$$

$$z - z''_0 = |z - z''_0| \exp(i\gamma), \quad z - \ell = |z - \ell| \exp(-i\alpha) \quad (9)$$

(see Fig. 2). Hence, the energy h and the stream function ψ are

$$h_\infty = K_\infty^{-1} \left[\mathcal{Q} \ln \left(\frac{|z|}{|z - \ell|} \right) + Q_\infty \ln \left(\frac{|z - z'_0|}{|z - z''_0|} \right) + \operatorname{Re}(C_\infty) \right], \quad (10)$$

$$h_0 = K_0^{-1} \left[Q_0 \ln \left(\frac{|z|}{|z - \ell|} \right) + \operatorname{Re}(C_0) \right], \quad (11)$$

and

$$\psi_\infty = \mathcal{Q}(\vartheta - \alpha) + Q_\infty(\gamma - \beta) + \operatorname{Im}(C_\infty), \quad (12)$$

$$\psi_0 = Q_0(\vartheta - \alpha) + \operatorname{Im}(C_0), \quad (13)$$

respectively. Then, the requirement of the (i) and (ii) conditions leads to

$$(\kappa \mathcal{Q} - Q_0) \ln \left(\frac{|z|}{|z - \ell|} \right) + \kappa Q_\infty \ln \left(\frac{|z - z'_0|}{|z - z''_0|} \right) = \text{Re}(C_0 - \kappa C_\infty), \quad (14)$$

$$(\mathcal{Q} - Q_0)(\vartheta - \alpha) + Q_\infty(\gamma - \beta) = \text{Im}(C_0 - C_\infty), \quad (15)$$

where we have introduced the ‘‘contrast ratio’’ $\kappa = K_0/K_\infty$. Since, according to the circle theorem, z'_0 and O are inverse points, it results $|z_0 - z'_0||z_0| = |z - z_0|^2$, and concurrently triangles of vertexes $\{z, z_0, z'_0\}$ and $\{z, z_0, O\}$ are similar (inversion theorem). By the same reasoning, triangles of vertexes $\{z, z_0, z''_0\}$ and $\{z, z_0, \ell\}$ are also similar. Hence, application of the law of sines finally leads to

$$\frac{|z|}{|z - \ell|} = \frac{|z_0|}{|z_0 - \ell|} \frac{|z - z'_0|}{|z - z''_0|}, \quad z \in \partial\Omega_0. \quad (16)$$

Insertion of (16) into (14), and taking the constants C_0 and C_∞ such that $\text{Re}(C_0 - \kappa C_\infty) = (\kappa \mathcal{Q} - Q_0) \ln(|z_0|/|z_0 - \ell|)$, provides a first equation $Q_0 = \kappa(\mathcal{Q} + Q_\infty)$. A second equation is obtained by noting that, from the triangle of vertexes $\{O, z, \ell\}$, it yields

$$\gamma - \beta - \pi = -(\vartheta - \alpha), \quad z \in \partial\Omega_0 \quad (17)$$

(Fig. 2). Substitution of (17) into (15), and selecting $\text{Im}(C_0 - C_\infty) = \pi Q_\infty$, gives $Q_0 = \mathcal{Q} - Q_\infty$. This latter, together with the one above, gives

$$Q_\infty = \frac{1 - \kappa}{1 + \kappa} \mathcal{Q}, \quad Q_0 = \frac{2\kappa}{1 + \kappa} \mathcal{Q}. \quad (18)$$

Finally, the left constants C_∞ and C_0 can be determined once one of these [the other is computed according to the conditions leading to Eqs. (18)] is fixed. In particular, the algebra simplifies tremendously by requiring that $w_0(z_0) = Q_0 \ln[z_0/(z_0 - \ell)]$. As a consequence, $C_0 = 0$ and one has $C_\infty = (\ln |z_0| - \ln |z_0 - \ell| - i\pi)Q_\infty$. Hence, potentials (4) and (5) are determined uniquely, and they ultimately write as

$$h(\mathbf{x}) = \frac{\mathcal{Q}}{K_\infty} \begin{cases} \ln \left(\frac{|z|}{|z - \ell|} \right) + \frac{1 - \kappa}{1 + \kappa} \ln \left(\frac{|z_0|}{|z_0 - \ell|} \frac{|z - z'_0|}{|z - z''_0|} \right), & \mathbf{x} \in \Omega_\infty, \\ \frac{2}{1 + \kappa} \ln \left(\frac{|z|}{|z - \ell|} \right), & \mathbf{x} \in \Omega_0, \end{cases}$$

$$\psi(\mathbf{x}) = \mathcal{Q} \begin{cases} \vartheta - \alpha + \frac{1 - \kappa}{1 + \kappa}(\gamma - \beta - \pi), & \mathbf{x} \in \Omega_\infty, \\ \frac{2\kappa}{1 + \kappa}(\vartheta - \alpha), & \mathbf{x} \in \Omega_0. \end{cases} \quad (19)$$

The analytical expressions (19) of the specific energy h and stream function ψ represent one of the main results of the present study. In particular, for $\kappa = 1$ (i.e., $K_0 = K_\infty$) one recovers the well known result valid for homogeneous media. In addition, $\kappa = 0$ provides the solution pertaining to an impermeable inclusion (see, e.g., [17]), and therefore Eqs. (19) constitute a generalization of previous results. In Fig. 3, we have depicted the nondimensional contour plot (red dashed lines) of hK_∞/\mathcal{Q} . It is seen that for $\kappa \ll 1$ levels of h are quite dense within Ω_0 , whereas the shape of the isovalues is completely reversed (i.e., they are repelled by the inclusion) for $\kappa \gg 1$.

The expressions (19) constitute the basis to tackle more complex problems concerning dipole-flow within disordered (typically porous) media. In particular, the remainder of the paper is devoted to the implementation of the above analytical results to compute the effective conductivity.

III. EFFECTIVE CONDUCTIVITY

So far, the flow domain Ω_∞ has been considered homogeneous (constant conductivity). However, this picture appears too simplistic as far as natural formations are concerned. In porous media, it is in fact a rule, rather than the exception, that the conductivity is varying in the space into an erratic manner, therefore defying any attempt to regard it as a constant. In order to account for these erratic

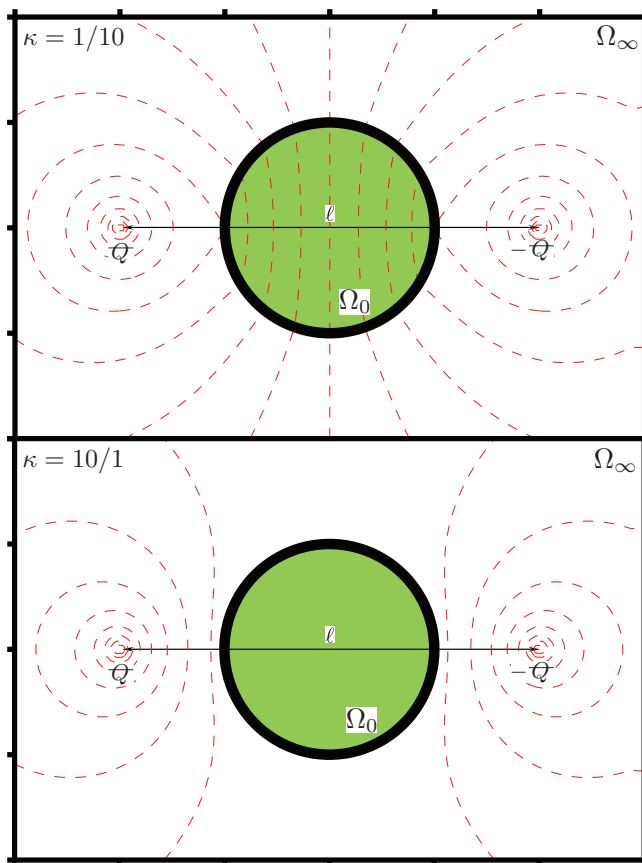


FIG. 3. Contour plot of the scaled hydraulic head hK_∞/\mathcal{Q} for two largely different values of the contrast ratio $\kappa = K_0/K_\infty$. The center of the inclusion (whose radius is $\mathcal{R}_0 = \ell/4$) is placed between the sink and the source.

variations and the associated uncertainty, it is customary to regard the natural logarithm Y of the conductivity as a stationary, Gaussian, random field [18]. In general, modeling Y as a random field is equivalent to the approach adopted in a large variety of turbulent flows, such as flow in pipelines, density-driven flows, flow through pumps and turbines, and reactive flows (a wide review can be found in [19]). The difference is that in turbulent flows the random nature of the depending scalar field is due to the velocity which is regarded as a given random field, whereas in the present study the random nature of the flow variables stems from the spatial variability of the conductivity.

Before proceeding further, we wish to briefly discuss the pertinency of a two-dimensional approach (considered in the present study) to mimic a flow pattern that, in the presence of wells, is generally three-dimensional. In this case, the requirement is that streamlines are linear [20,21]: a condition which is certainly met in absence of well screening and if the well is fully penetrating (see, e.g., [22,23]). Likewise, at the regional scale [24], if the well is fully penetrating and the aquifer's thickness is small as compared to relevant horizontal length scale for the problem at stake, one can resort with a two-dimensional approach. Hence, the modeling approach employed in the sequel is relevant not only from the theoretical point of view, but also for the practical applications.

A central question in the theory of heterogeneous media is whether one can define an effective constitutive law even when flow is driven by a system of isolated and/or distributed sources. While this topic is well established in the case of a flow driven by a uniform mean velocity (see [25], and references therein), to our knowledge there are no studies dealing with the analogous problem for a dipole-flow. In the case of flow driven by a single source, Ref. [8] has recently derived the EC, relating the mean flux $\langle \mathbf{q} \rangle$ to the mean gradient $\nabla \langle h \rangle$ in the Darcy law, i.e., $\langle \mathbf{q} \rangle = -\mathbf{K}^{\text{eff}} \nabla \langle h \rangle$. The important result is that the EC is position-dependent.

In the present study, we generalize such an approach to account for a system of sink/source. Toward this aim, we adhere to the standpoint of the SCA [26]: the porous formation is sought as a collection of a large number \mathcal{N} of randomly arranged, homogeneous, non-overlapping circular inclusions of different conductivity values. Generally, a two-dimensional formation exhibits horizontal integral scales of the same size (see, e.g., Tables 2.1 and 2.2 in [18]), and therefore Y is regarded as an isotropic random field. In this case, the use of circular inclusion is not limiting, since it leads to results which match very well numerical simulations [27,28]. Instead, if one deals with the vertical heterogeneity, the conductivity exhibits a vertical integral scale lesser than the horizontal one. As a consequence, the heterogeneity structure is anisotropic, and adopting inclusions like ellipses would be worthwhile (for details, see, e.g., [29–31], and references therein). Then, by recalling that the flow domain is large enough to apply ergodicity to the conductivity values (details about the attainment of such a requirement are discussed by [24]), one can replace the actual formation with the ensemble average, and therefore the simultaneous interaction among the numerous inclusions can be approached by focusing upon a single one implanted into a medium homogenized by a background. It is therefore clear that, in order to apply the SCA to a dipole, solving the flow in the configuration of Fig. 1 becomes the crucial prerequisite. For this single realization, we consider the actual flux \mathbf{q} as disturbed by the inclusion Ω_0 of conductivity $K_0 \neq K_\infty$, and center at $|z_0| \equiv r_0$. Thus, the fluctuation \mathbf{q}' is obtained by means of the Reynolds decomposition as

$$\mathbf{q}'(\mathbf{x}) = \mathbf{q}(\mathbf{x}) - \mathbf{q}_\infty(\mathbf{x}), \quad (20)$$

being $\mathbf{q}_\infty(\mathbf{x}) = -K_\infty \nabla h(\mathbf{x})$ the flux of the background Ω_∞ where, unlike the deterministic case, now K_∞ is left unknown. Decomposition (20) is then averaged over all possible positions, sizes, and conductivities to come up with

$$\langle \mathbf{q}(\mathbf{x}) \rangle = -K_\infty \nabla \langle h(\mathbf{x}) \rangle + \langle \mathbf{q}'(\mathbf{x}) \rangle. \quad (21)$$

From this latter, it is seen that to apply the SCA, one has to require that $\langle \mathbf{q}' \rangle \equiv \mathbf{0}$ throughout the flow domain Ω_∞ . In a different manner, the EC is such to compensate (in the ensemble average sense) the deviation of the flux from the mean value. This methodology is bound to be accurate if (i) interactions between inclusions are neglected, (ii) blocks are circles, and (iii) the domain is much larger than the single inclusions. In particular, due to the assumption of total randomness of the location of the inclusion, the ensemble average over the position is replaced by a spatial integration over a large circle Ω_R of radius $R \gg r_0$ surrounding Ω_0 , i.e.,

$$\frac{1}{\Omega_R} \int_{\Omega_R} d\mathbf{x} \mathbf{q}'(\mathbf{x}) = \frac{1}{\Omega_R} \int_{\Omega_0} d\mathbf{x} [\mathbf{q}'_0(\mathbf{x}) - \mathbf{q}'_\infty(\mathbf{x})] + \frac{1}{\Omega_R} \int_{\Omega_R} d\mathbf{x} \mathbf{q}'_\infty(\mathbf{x}), \quad (22)$$

where we have set

$$\mathbf{q}'_\infty(\mathbf{x}) = -\mathcal{Q} \frac{1-\kappa}{1+\kappa} \nabla f_\infty(\mathbf{x}), \quad \mathbf{q}'_0(\mathbf{x}) = \mathcal{Q} \frac{1-\kappa}{1+\kappa} \nabla f_0(\mathbf{x}), \quad (23)$$

$$f_\infty(\mathbf{x}) \equiv \ln \left(\frac{|\mathbf{x} - \mathbf{x}'_0|}{|\mathbf{x} - \mathbf{x}''_0|} \right), \quad f_0(\mathbf{x}) \equiv \ln \left(\frac{|\mathbf{x}|}{|\mathbf{x} - \boldsymbol{\ell}|} \right), \quad (24)$$

$$\mathbf{x}'_0 \equiv (\text{Re } z'_0, \text{Im } z'_0), \quad \mathbf{x}''_0 \equiv (\text{Re } z''_0, \text{Im } z''_0), \quad \boldsymbol{\ell} \equiv (\ell, 0). \quad (25)$$

Thus, application of the SCA leads to the following general result:

$$\left\langle \frac{K^{\text{eff}} - K_0}{K^{\text{eff}} + K_0} \Lambda_i(\mathcal{R}_0, \mathbf{r}_0) \right\rangle = 0, \quad (i = 1, 2), \quad (26)$$

being

$$\Lambda_i(\mathcal{R}_0, \mathbf{r}_0) \stackrel{R \rightarrow \infty}{=} \frac{1}{\Omega_R} \int_{\Omega_0} d\mathbf{x} \frac{\partial}{\partial x_i} [f_0(\mathbf{x}) + f_\infty(\mathbf{x})] + \frac{1}{\Omega_R} \int_{\Omega_R} d\mathbf{x} \frac{\partial}{\partial x_i} f_\infty(\mathbf{x}). \quad (27)$$

The algebraic equations (26) enable one to compute the two components of the EC, once the joint probability distribution $f \equiv f(K_0, \mathcal{R}_0, \mathbf{r}_0)$ is selected. The most important feature, which is detected from inspection of (26), is the dependence of the EC upon the configuration through the terms (27), a feature which prevents *de facto* considering K^{eff} as a local medium's property. However, if K_0 and $(\mathcal{R}_0, \mathbf{r}_0)$ are uncorrelated random fields, from Eq. (26) it yields

$$\left\langle \frac{K^{\text{eff}} - K_0}{K^{\text{eff}} + K_0} \right\rangle = 0, \quad (28)$$

whose solution is the geometric mean, i.e., $K^{\text{eff}} \equiv K_G = \exp\langle Y \rangle$ (in agreement with [32]). In this case, one can regard K^{eff} as a medium's property (similarly to a mean uniform flow [24]), and concurrently dipole-flow can be solved by superimposing two single sources of opposite strength, with the conductivity K_∞ replaced by K_G .

Turning to Eqs. (26), the evaluation of the integrals appearing on the right-hand side of (27) is achieved by means of the Green's theorem, and the final result is

$$\Lambda_i \stackrel{R \rightarrow \infty}{=} 2n_0 \begin{cases} r_0^{-1}, & i = 1, \\ |\mathbf{r}_0 - \boldsymbol{\ell}|^{-1}, & i = 2, \end{cases} \quad (29)$$

being the ratio $n_0 \equiv \Omega_0/\Omega_R$ equal, in the limit $\mathcal{N} \rightarrow \infty$, to $f(K_0, \mathcal{R}_0) dK_0 d\mathcal{R}_0$. For fixed \mathbf{r}_0 , Eqs. (26), together with (29), are grouped into a single one (accounting for the fact that the inclusion's radius \mathcal{R}_0 is required to be lesser than $\min\{r_0, |\boldsymbol{\ell} - \mathbf{r}_0|\} \equiv r_<$) as follows:

$$\int_0^\infty \int_0^{r_<} dK_0 d\mathcal{R}_0 f(K_0, \mathcal{R}_0) \frac{K^{\text{eff}} - K_0}{K^{\text{eff}} + K_0} = 0. \quad (30)$$

In particular, for $\ell \gg r_0$, the sink does not impact the near field, and in (30) one can replace $r_< \rightarrow r_0$, thus obtaining the equation for the EC valid for a flow generated by a single source (in agreement with [8]).

Based on field findings (a comprehensive review can be found in [18]), hereafter we shall assume that K_0 and \mathcal{R}_0 are both log-normally distributed (with correlation coefficient ρ). As a consequence, one quadrature appearing in (30) is easily carried out, leading to

$$\int_{-\infty}^{+\infty} dY' \exp\left(-\frac{Y'^2}{2\sigma_Y^2}\right) \frac{\kappa^{\text{eff}} - \exp Y'}{\kappa^{\text{eff}} + \exp Y'} \text{erfc}[\xi(Y')] = 0 \quad (31)$$

with $Y' = Y - \langle Y \rangle$ (fluctuation of $Y = \ln K_0$). In addition, we have set

$$\kappa^{\text{eff}} = \frac{K^{\text{eff}}}{K_G}, \quad \xi(u) = \frac{\rho u / \sigma_Y - Z_< / \sigma_Z}{\sqrt{2(1 - \rho^2)}}, \quad (32)$$

being $Z_< = \ln(r_</Z_G)$ the log-transform of $r_<$ normalized by the geometric mean of $Z = \ln \mathcal{R}_0$, whereas σ_Z^2 is the variance of Z . Likewise, K_G and σ_Y^2 are the geometric mean and variance of Y , respectively.

It is easy to check that the continuous function

$$\mathcal{F}(u) \equiv \int_{-\infty}^{+\infty} dY' \exp\left(-\frac{Y'^2}{2\sigma_Y^2}\right) \frac{u - \exp Y'}{u + \exp Y'} \text{erfc}[\xi(Y')] \quad (33)$$

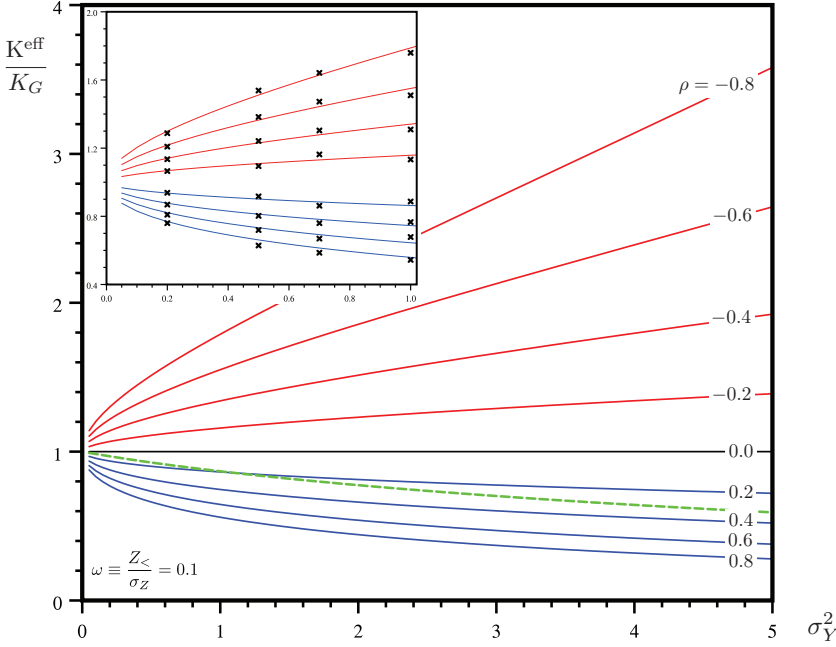


FIG. 4. Normalized EC as function of the variance σ_Y^2 , and several values of the correlation coefficient ρ . The EC pertaining to a mean uniform flow (green, thick, dashed line) is also shown. Other parameter: $\omega \equiv Z_{<}/\sigma_Z = 0.1$. The inset shows the comparison between numerical simulations (symbols) and analytical self-consistent model (lines) of the scaled EC.

is such that $\mathcal{F}(0) < 0$, $\mathcal{F}(+\infty) > 0$, and $\mathcal{F}'(u) > 0$ (any $u \in [0, +\infty[$). As a consequence, Eq. (31) admits a single solution κ^{eff} (to be searched numerically). Moreover, since (33) is a convex function of the u variable, one can consider the tangent to $\mathcal{F} \equiv \mathcal{F}(u)$ in the point $(0, \mathcal{F}(0))$ to obtain a lower bound, $\kappa_{\star}^{\text{eff}}$, of the normalized EC. The final result is

$$\kappa_{\star}^{\text{eff}} = -\frac{\mathcal{F}(0)}{\mathcal{F}'(0)}. \quad (34)$$

The bound (34) can be used to check the accuracy of more involved numerical codes (accounting, for instance, for complex boundary conditions). In addition, $\kappa_{\star}^{\text{eff}}$ has been used in the numerical solution of (31) leading to Fig. 4, showing K^{eff} (normalized by K_G) as function of σ_Y^2 , and several values of the correlation coefficient ρ . The left parameters are grouped in the term $\omega = Z_{<}/\sigma_Z$ which, for illustration purposes, is taken equal to 0.1 (similar conclusions are drawn for any other $\omega \in \mathbb{R}$). It is seen that a negative correlation (red lines in Fig. 4) is attached to an EC larger than the background K_G , whereas the opposite happens (blue lines in Fig. 4) for $\rho > 0$. In order to provide a mechanical explanation of such a behavior, we can focus on the pattern of the flow as determined by a single inclusion Ω_0 (see Fig. 3) embedded into a matrix of conductivity K_{∞} (being the EC computed over many of such realizations).

Starting with the case of negatively correlated $K_0 - \mathcal{R}_0$, we consider the behavior of the fluctuation \mathbf{q}' at a point $P_0 \in \Omega_{\infty}$, that is chosen close to the boundary $\partial\Omega_0$ of the inclusion (away from $\partial\Omega_0$ the background flow is not impacted by \mathbf{q}'). Thus, a reduction of \mathcal{R}_0 implies an increase of K_0 , and concurrently one has $\kappa > 1$. Hence, due to the mass conservation, isoheads become denser outside Ω_0 (Fig. 4), and therefore the fluctuation in P_0 (that still lays in Ω_{∞}) is such to reduce the background flux. As a consequence, the SCA requires the EC to increase in order to compensate the increment of the flux passing through Ω_0 . A similar argument applies for an increase of \mathcal{R}_0

determining a reduction of K_0 (i.e., $\kappa < 1$). Indeed, in this case P_0 now falls within the inclusion, where the fluctuation \mathbf{q}' reduces the flux there (due to the fact that Ω_0 behaves like a flow barrier). Again, the EC has to increase in order to meet the requirement of the SCA.

The same reasoning is adopted to explain why, for $\rho > 0$, the EC is less than K_G . In fact, in this case a reduction of \mathcal{R}_0 produces a reduction of K_0 ($\kappa < 1$), and concurrently the fluctuation \mathbf{q}' in P_0 (belonging to Ω_∞) produces an increment in the background flux. This determines a reduction of the EC as compared with that of the background K_G . Likewise, consider an increase of the inclusion's radius, corresponding to an increase in the conductivity K_0 ($\kappa > 1$). The point P_0 now belongs to Ω_0 , where the flux has increased (the density of the isohead values drastically reduces inside the inclusion), and again the EC reduces. For $\rho = 0$, one recovers the solution $\kappa^{\text{eff}} = 1$. Moreover, it is seen that the deviation of the EC from the geometric mean K_G increases/decreases with negative/positive ρ , respectively. For comparison purposes, in Fig. 4 we have also depicted (green, thick, dashed line) the normalized EC pertaining to a mean uniform flow (Eq. (45) in [33], with $m = 2$).

To assess the analytical results, numerical (Monte Carlo) simulations have been carried out, as well. The numerical (crossed symbols in the inset of Fig. 4) values of the scaled effective conductivity K^{eff}/K_G are found in a relatively good agreement with their analytical (continuous lines) counterparts. In particular, the Monte Carlo simulations are limited to $\sigma_Y^2 \leq 1$, since accounting for larger σ_Y^2 values would have demanded a very dense discretization of the flow domain, thus leading to an extremely large number of algebraic equations. In addition, a large Y variance rapidly deteriorates any numerical approximation of the Dirac pulse (no matter how efficient is its numerical approximation [34]). To conclude our discussion of the results, we wish to emphasize that the analytical solution (31), being based only upon the univariate probability density function of Y , relies on a quite robust, seldom met (see, e.g., field data in Tables 2.1 and 2.2 in [18]) assumption which allows one to avoid more sophisticated approaches, such as those based upon the concept of connectivity [35,36] or training images [37].

IV. CONCLUDING REMARKS

Steady dipole-flow through a porous medium of background conductivity K_∞ , and disturbed by a circular inclusion with $K_0 \neq K_\infty$, is solved here. The adopted method, relying upon a slight modification of the circle theorem [16], is fairly general and therefore it can be adopted for other flow configurations, as well.

We have derived a closed-form solution for the potential, consisting of (i) the potential pertaining to the homogeneous domain, and (ii) a paired (fictitious) source/sink system lying inside the inclusion, in order to account for the mass and energy conservation on the boundary of the inclusion. The analytical solution is exact (no approximation or perturbations are employed), and it contains the solutions of flow disturbed by an inclusion of zero conductivity as a particular case.

Besides the theoretical interest, our analytical solution provides a way of modeling the stochastic heterogeneity of aquifers by means of the SCA. Thus, we have focused on the computation of the effective conductivity, a topic which has been intensively studied for mean uniform flows, and only recently it has been applied to flows generated by a single source.

The EC is derived by assuming the following: (i) The matrix surrounding each inclusion is replaced by a homogeneous background of conductivity K_∞ . Such an approximation is bound to be quite accurate if interactions between blocks are negligible. (ii) Inclusions are circular, which is a quite accurate approximation for an isotropic medium. (iii) The domain is large compared to that of the inclusion, in order to invoke ergodicity. Although assumptions (i)–(iii) are clearly an approximation, they nevertheless do not limit the accuracy of the final result, as was assessed by [28] by means of very accurate numerical simulations.

The main result is that the EC is not generally a medium's property (nonlocality). In particular, the EC is found lower/larger than the background K_G if the coefficient of correlation ρ between the conductivity and the position of the inclusions making up the porous medium is positive/negative,

respectively. This is explained straightforwardly as a consequence of the mass conservation at the boundary of the inclusion.

Our results find application in the numerical study of the advective transport through strongly heterogeneous (large σ_Y^2) porous formations. Not disregarded, they can also be used as a benchmark to validate more involved (accounting, for instance, for the presence of boundaries) numerical codes [38,39].

ACKNOWLEDGMENTS

The present study was developed within the GNCS (Gruppo Nazionale Calcolo Scientifico - INdAM) framework. We thank the associate editor and the two referees for their comments, which have significantly improved the early version of the manuscript.

-
- [1] H. S. Carslaw and J. C. Jaeger, *Conduction of Heat in Solids* (Oxford Science Publications, Oxford, 2000).
 - [2] J. D. Jackson, *Classical Electrodynamics* (John Wiley & Sons, New York, 2007).
 - [3] A. Zech, C. D'Angelo, S. Attinger, and A. Fiori, Revisitation of the dipole tracer test for heterogeneous porous formations, *Adv. Water Resour.* **115**, 198 (2018).
 - [4] M. Di Dato, F. P. de Barros, A. Fiori, and A. Bellin, Improving the efficiency of 3-d hydrogeological mixers: Dilution enhancement via coupled engineering-induced transient flows and spatial heterogeneity, *Water Resour. Res.* **54**, 2095 (2018).
 - [5] G. Severino, Dispersion in doublet-type flows through highly anisotropic porous formations, *J. Fluid Mech.* **931**, A2 (2022).
 - [6] A. Chamolly and E. Lauga, Stokes flow due to point torques and sources in a spherical geometry, *Phys. Rev. Fluids* **5**, 074202 (2020).
 - [7] P. G. Ledda, L. Siconolfi, F. Viola, F. Gallaire, and S. Camarri, Suppression of von Karman vortex streets past porous rectangular cylinders, *Phys. Rev. Fluids* **3**, 103901 (2018).
 - [8] G. Severino, Effective conductivity in steady well-type flows through porous formations, *Stochastic Environmental Research and Risk Assessment* **33**, 827 (2019).
 - [9] S. W. Wheatcraft and F. Winterberg, Steady state flow passing through a cylinder of permeability different from the surrounding medium, *Water Resour. Res.* **21**, 1923 (1985).
 - [10] P. Meliga, Computing the sensitivity of drag and lift in flow past a circular cylinder: Time-stepping versus self-consistent analysis, *Phys. Rev. Fluids* **2**, 073905 (2017).
 - [11] M. Sahimi, *Heterogeneous Materials I: Linear Transport and Optical Properties* (Springer Science & Business Media, 2003).
 - [12] B. Noetinger, L. Hume, R. Chatelin, and P. Poncet, Effective viscosity of a random mixture of fluids, *Phys. Rev. Fluids* **3**, 014103 (2018).
 - [13] J. Koplik, S. Redner, and E. Hinch, Tracer dispersion in planar multipole flows, *Phys. Rev. E* **50**, 4650 (1994).
 - [14] P. Kurowski, I. Ippolito, J. Hulin, J. Koplik, and E. Hinch, Anomalous dispersion in a dipole flow geometry, *Phys. Fluids* **6**, 108 (1994).
 - [15] M. Bianchi, C. Zheng, G. R. Tick, and S. M. Gorelick, Investigation of small-scale preferential flow with a forced-gradient tracer test, *Groundwater* **49**, 503 (2011).
 - [16] L. M. Milne-Thomson, *Theoretical Hydrodynamics* (Courier Corporation, 1968).
 - [17] G. A. Bruggeman, *Analytical Solutions of Geohydrological Problems* (Elsevier, Amsterdam, 1999).
 - [18] Y. Rubin, *Applied Stochastic Hydrogeology* (Oxford University Press, 2003).
 - [19] S. B. Pope, *Turbulent Flows* (Cambridge, 2010).
 - [20] G. Dagan and S. C. Lessoff, Transmissivity upscaling in numerical aquifer models of steady well flow: Unconditional statistics, *Water Resour. Res.* **43**, W054311 (2007),.
 - [21] G. Dagan, S. C. Lessoff, and A. Fiori, Is transmissivity a meaningful property of natural formations? Conceptual issues and model development, *Water Resour. Res.* **45**, W03425 (2009).

- [22] D. Fernández-García, T. H. Illangasekare, and H. Rajaram, Conservative and sorptive forced-gradient and uniform flow tracer tests in a three-dimensional laboratory test aquifer, [Water Resour. Res.](#) **40**, W10103 (2004).
- [23] D. Fernandez-Garcia, X. Sánchez-Vila, and T. H. Illangasekare, Convergent-flow tracer tests in heterogeneous media: Combined experimental-numerical analysis for determination of equivalent transport parameters, [J. Contam. Hydrol.](#) **57**, 129 (2002).
- [24] G. Dagan, *Flow and Transport in Porous Formations* (Springer, 1989).
- [25] S. Torquato, *Random Heterogeneous Materials: Microstructure and Macroscopic Properties* (Springer Science & Business Media, 2013).
- [26] S. Kanaun and V. Levin, *Self-Consistent Methods for Composites: Static Problems* (Springer Science & Business Media, 2007).
- [27] A. Fiori, I. Jankovic, and G. Dagan, Effective Conductivity of Heterogeneous Multiphase Media with Circular Inclusions, [Phys. Rev. Lett.](#) **94**, 224502 (2005).
- [28] I. Jankovic, A. Fiori, and G. Dagan, Effective conductivity of an isotropic heterogeneous medium of lognormal conductivity distribution, [Multiscale Model. Simul.](#) **1**, 40 (2003).
- [29] G. Dagan and A. Fiori, Time-dependent transport in heterogeneous formations of bimodal structures: 1. The model, [Water Resour. Res.](#) **39**, 1112 (2003).
- [30] G. Dagan and S. Lessoff, Solute transport in heterogeneous formations of bimodal conductivity distribution: 1. Theory, [Water Resour. Res.](#) **37**, 465 (2001).
- [31] A. Fiori and G. Dagan, Time-dependent transport in heterogeneous formations of bimodal structures: 2. Results, [Water Resour. Res.](#) **39**, 1125 (2003).
- [32] P. Indelman, Averaging of unsteady flows in heterogeneous media of stationary conductivity, [J. Fluid Mech.](#) **310**, 39 (1996).
- [33] G. Dagan, Models of groundwater flow in statistically homogeneous porous formations, [Water Resour. Res.](#) **15**, 47 (1979).
- [34] V. Schiano Di Cola, S. Cuomo, and G. Severino, Remarks on the numerical approximation of Dirac delta functions, [Results in Applied Mathematics](#) **12**, 100200 (2021).
- [35] A. Fiori, F. Boso, F. P. de Barros, S. De Bartolo, A. Frampton, G. Severino, S. Suweis, and G. Dagan, An indirect assessment on the impact of connectivity of conductivity classes upon longitudinal asymptotic macrodispersivity, [Water Resour. Res.](#) **46**, W08601 (2010).
- [36] A. Zarlenga, I. Janković, A. Fiori, and G. Dagan, Effective hydraulic conductivity of three-dimensional heterogeneous formations of lognormal permeability distribution: The impact of connectivity, [Water Resour. Res.](#) **54**, 2480 (2018).
- [37] K. Mahmud, G. Mariethoz, A. Baker, and A. Sharma, Integrating multiple scales of hydraulic conductivity measurements in training image-based stochastic models, [Water Resour. Res.](#) **51**, 465 (2015).
- [38] P. Indelman, Steady-state source flow in heterogeneous porous media, [Transp. Porous Media](#) **45**, 105 (2001).
- [39] G. Severino, Stochastic analysis of well-type flows in randomly heterogeneous porous formations, [Water Resour. Res.](#) **47**, W03520 (2011).